Title: Diffractive Lensing of Gravitational Waves as a New Probe of Dark Matter

Speakers: Mesut Çalışkan

Collection/Series: Strong Gravity

Subject: Strong Gravity

Date: November 27, 2025 - 6:00 PM

URL: https://pirsa.org/25110122

Abstract:

Lensed gravitational waves (GWs) offer a promising new probe of dark matter. Dark matter subhalos can lens GWs from stellar-mass or massive black hole binaries, producing diffractive (wave-optics) lensing signatures in their chirping waveforms.

I will begin by highlighting how GW lensing differs from the lensing of light, particularly in its sensitivity to small-scale structure through frequency-dependent diffraction patterns. I will then discuss how these diffractive features encode the mass and density profile of dark matter subhalos, and how the rate of such events can inform their abundance. I will assess the detection prospects for current and upcoming GW detectors, and conclude by outlining key theoretical and computational challenges that must be addressed to advance this emerging probe.

Diffractive Lensing of Gravitational Waves as a New Probe of Dark Matter*

Mesut Çalışkan[1,α]

[1]*Johns Hopkins University*

Perimeter Institute, Strong Gravity Seminar – 27 November 2025

[α] caliskan@jhu.edu

* arXiv: 2201.04619, 2206.02803, 2307.06990

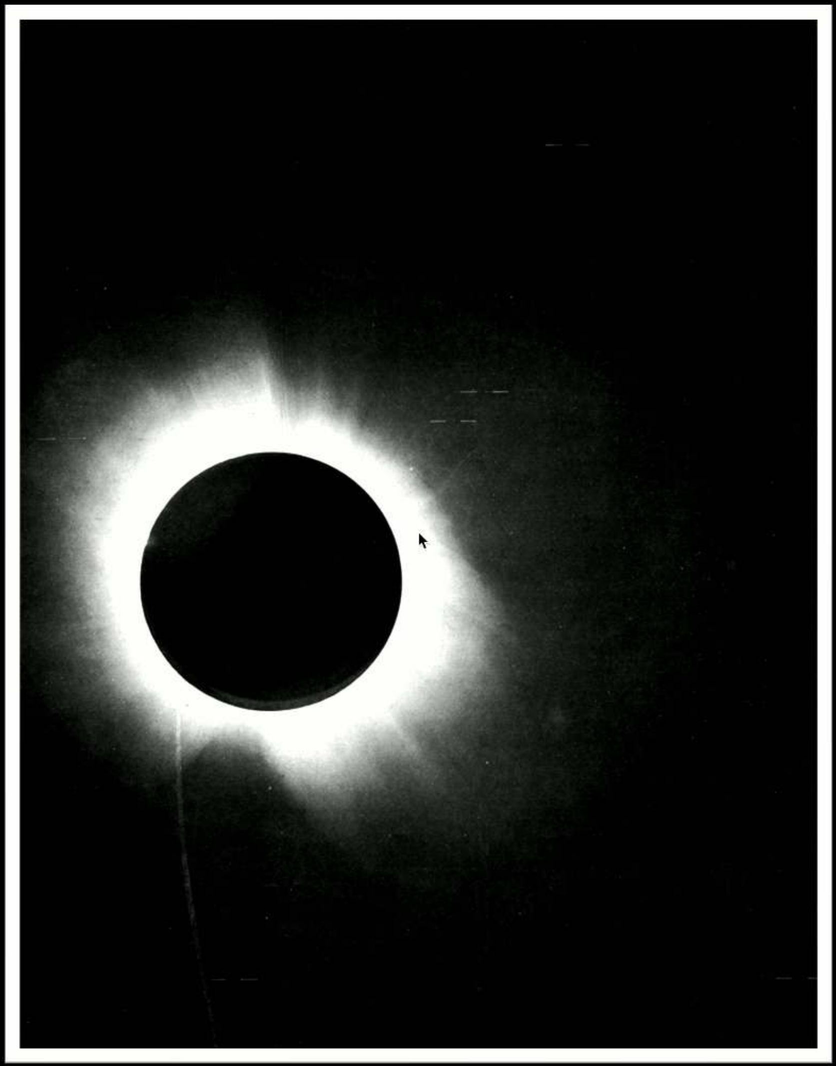

F. W. Dyson, A. S. Eddington, and C. Davidson (1920)

Current techniques are limited to probing dark-matter structures heavier than $\sim 10^8\ M_\odot$.

Probing the substructures within DM halos remains challenging because of their faint luminosity and low masses, which lead to much lower detection probabilities.

Testbed for the Nature of Dark Matter

Dark Matter

Gravitational Waves

Mass

Profile

Number Density

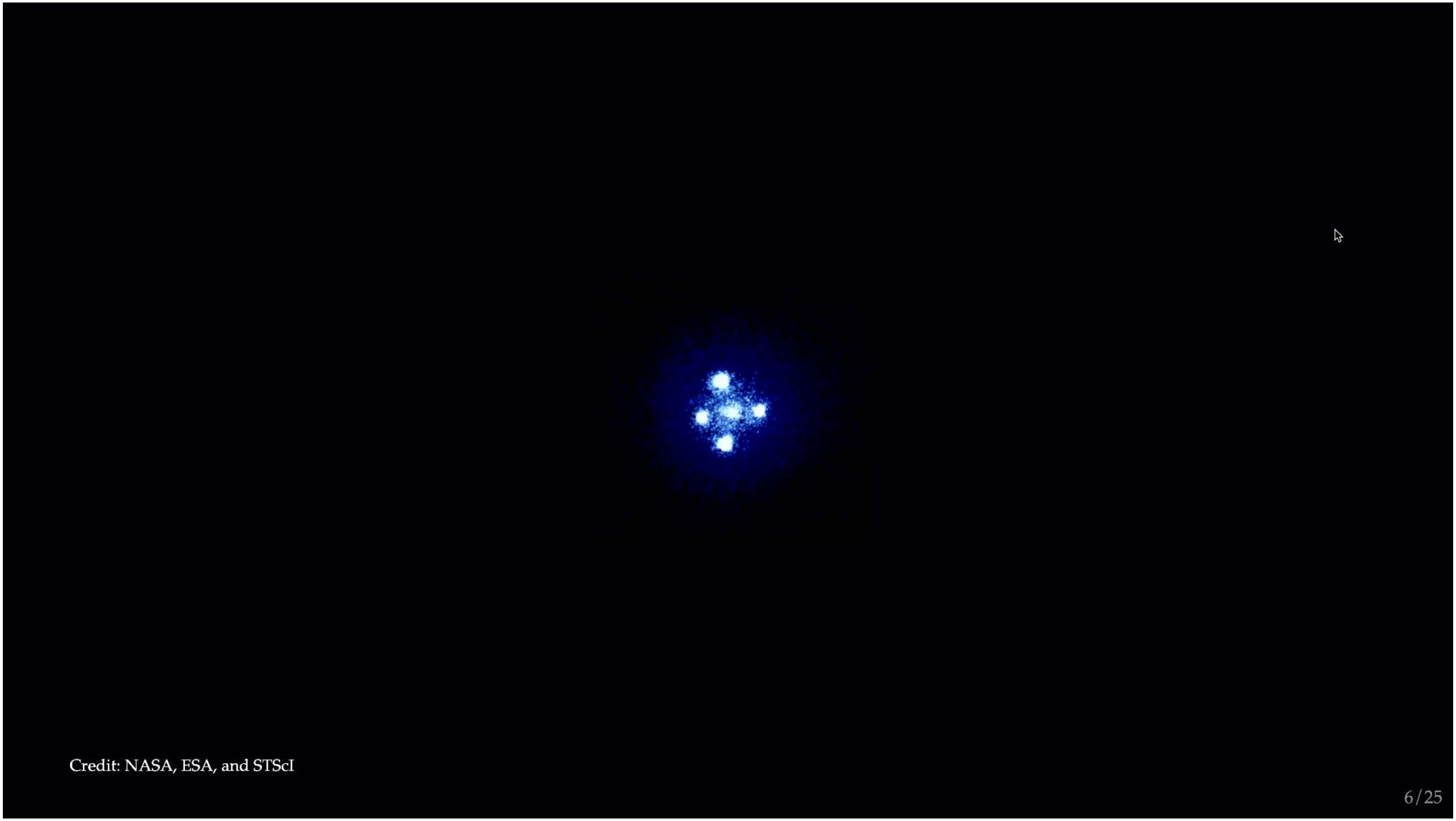

Credit: NASA, ESA, and STScI

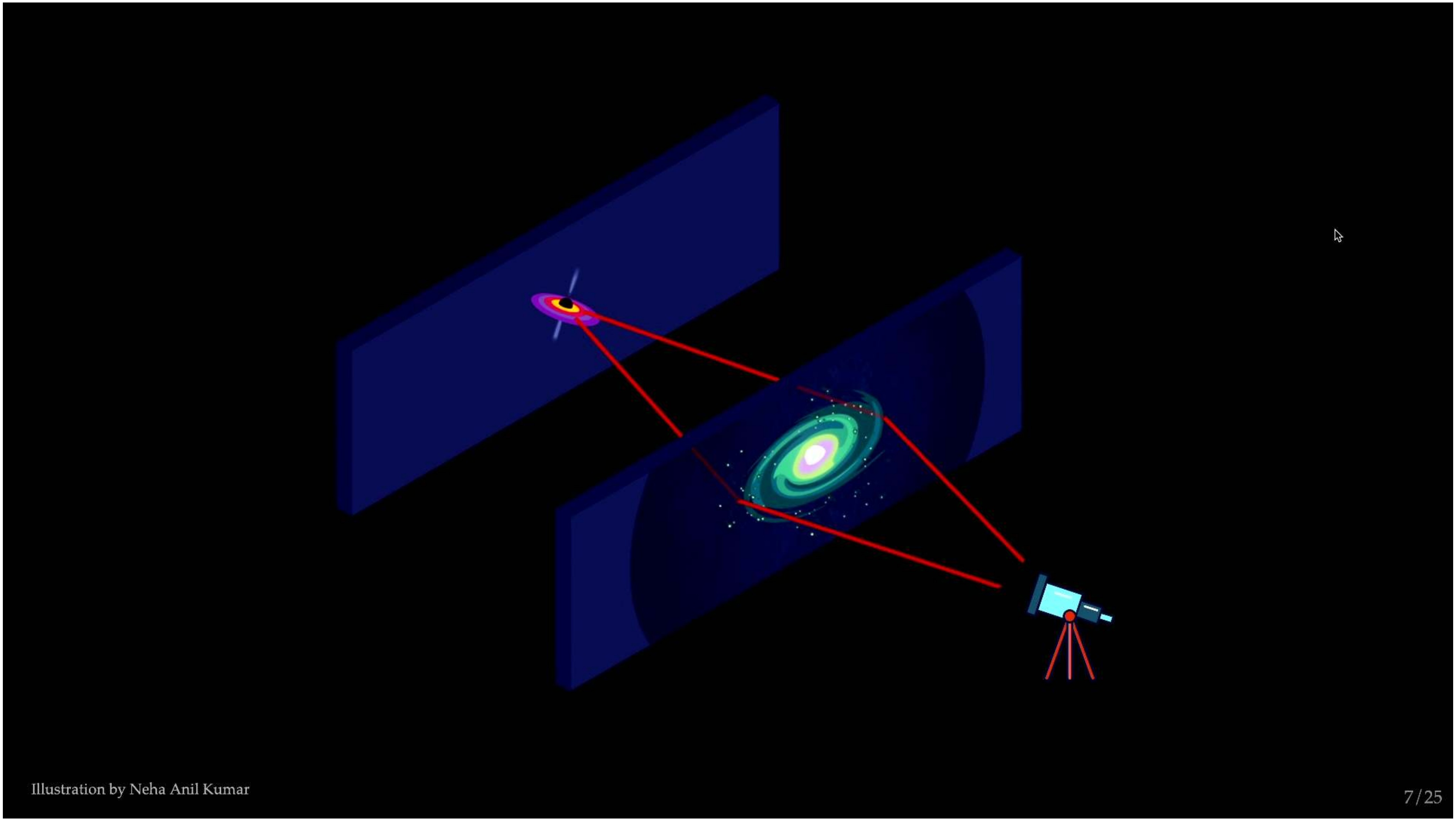
Illustration by Neha Anil Kumar
7 / 25

What if the source is a (massive) binary black hole?

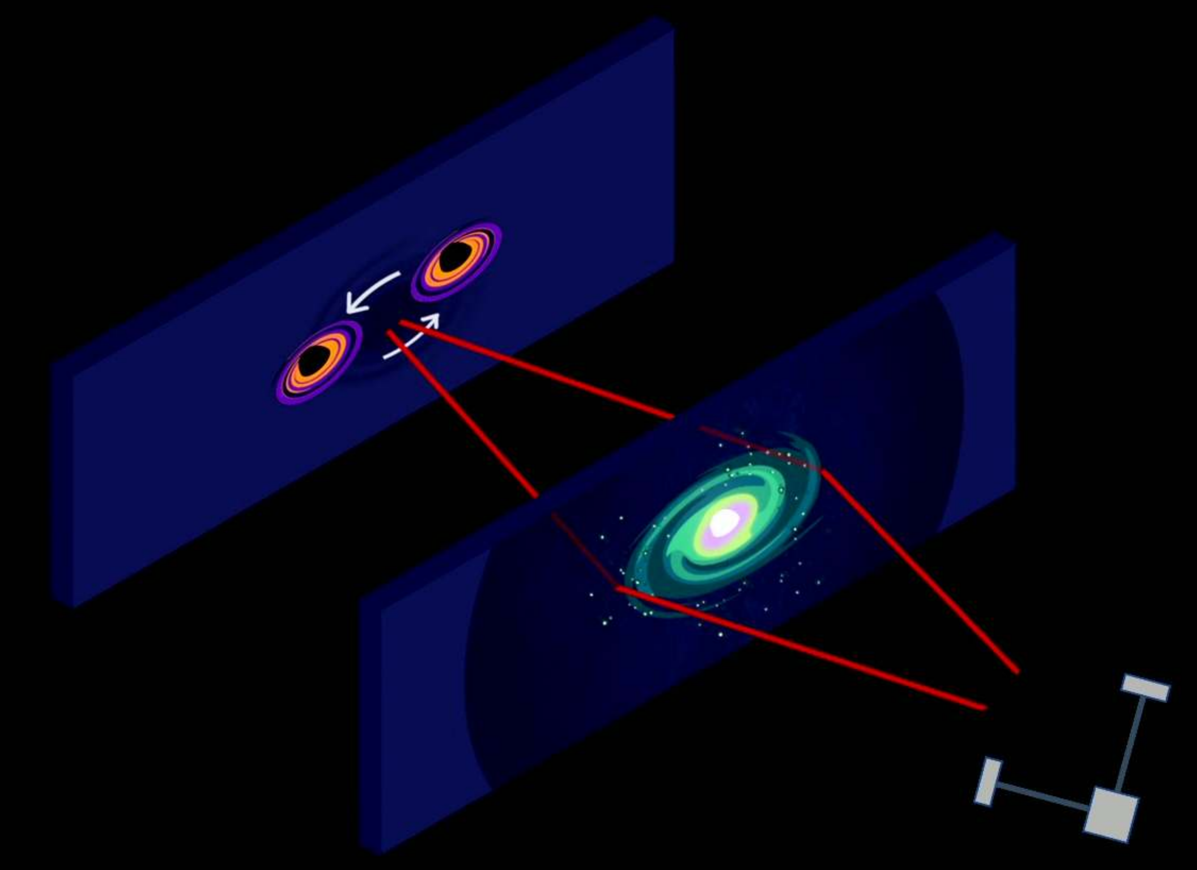

Illustration by Neha Anil Kumar

Unlensed Waveform

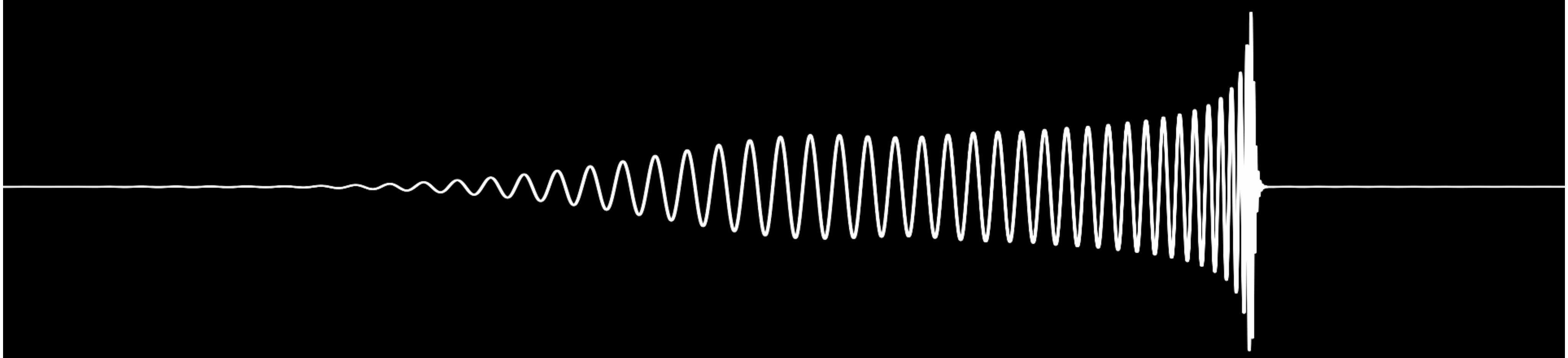

Strongly Lensed Waveforms

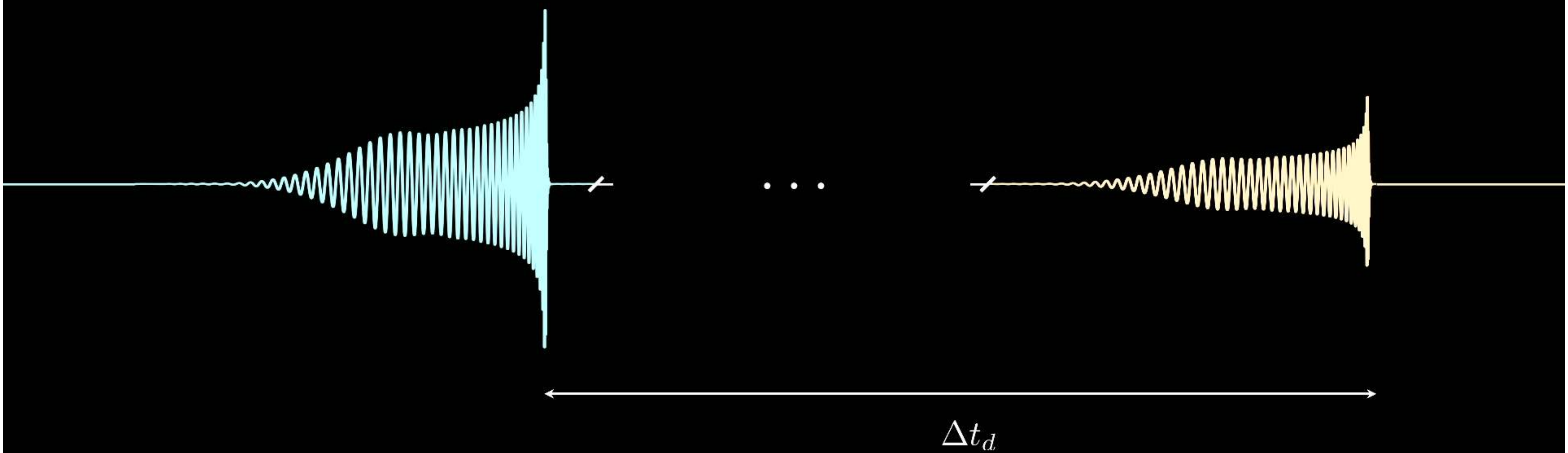

10 / 25

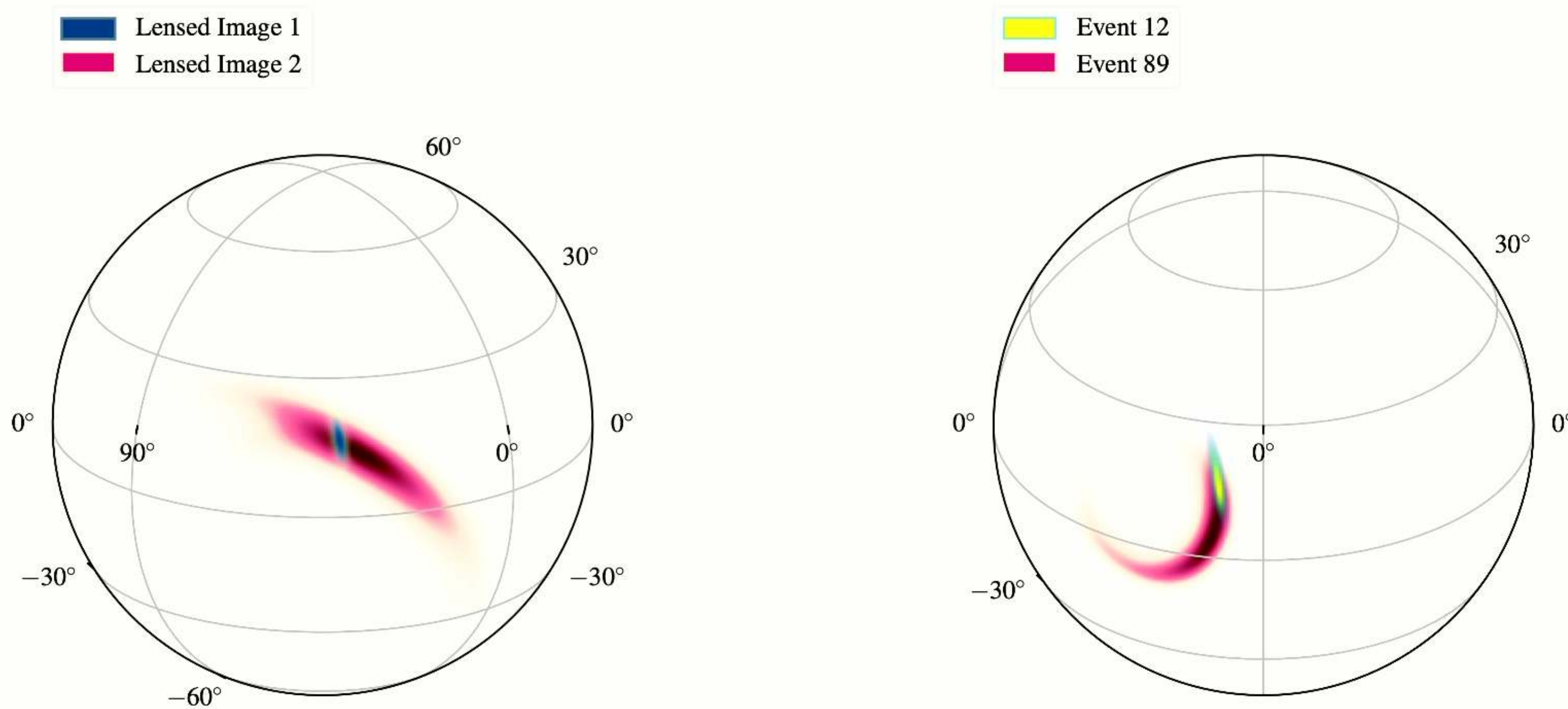

(a) lensed

(b) not lensed

[2] **Çalışkan** et al. (2022)

False Alarm Probability

$$\sim \frac{1}{10^4}$$

[2] **Çalışkan** et al. (2022)

Strong Lensing Rate?

$$\sim \frac{1}{10^3}$$

Li et al. (2018)

$$N_{\text{lensed}} \propto N_{\text{events}}$$

$$N_{\text{false alarms}} \propto N_{\text{events}}^2$$

[2] **Çalışkan** et al. (2022)

What if the lens is smaller?

Wave-Optics Effects

$$M_L \lesssim 10^5\, M_\odot \left(\frac{f}{\mathrm{Hz}}\right)^{-1}$$

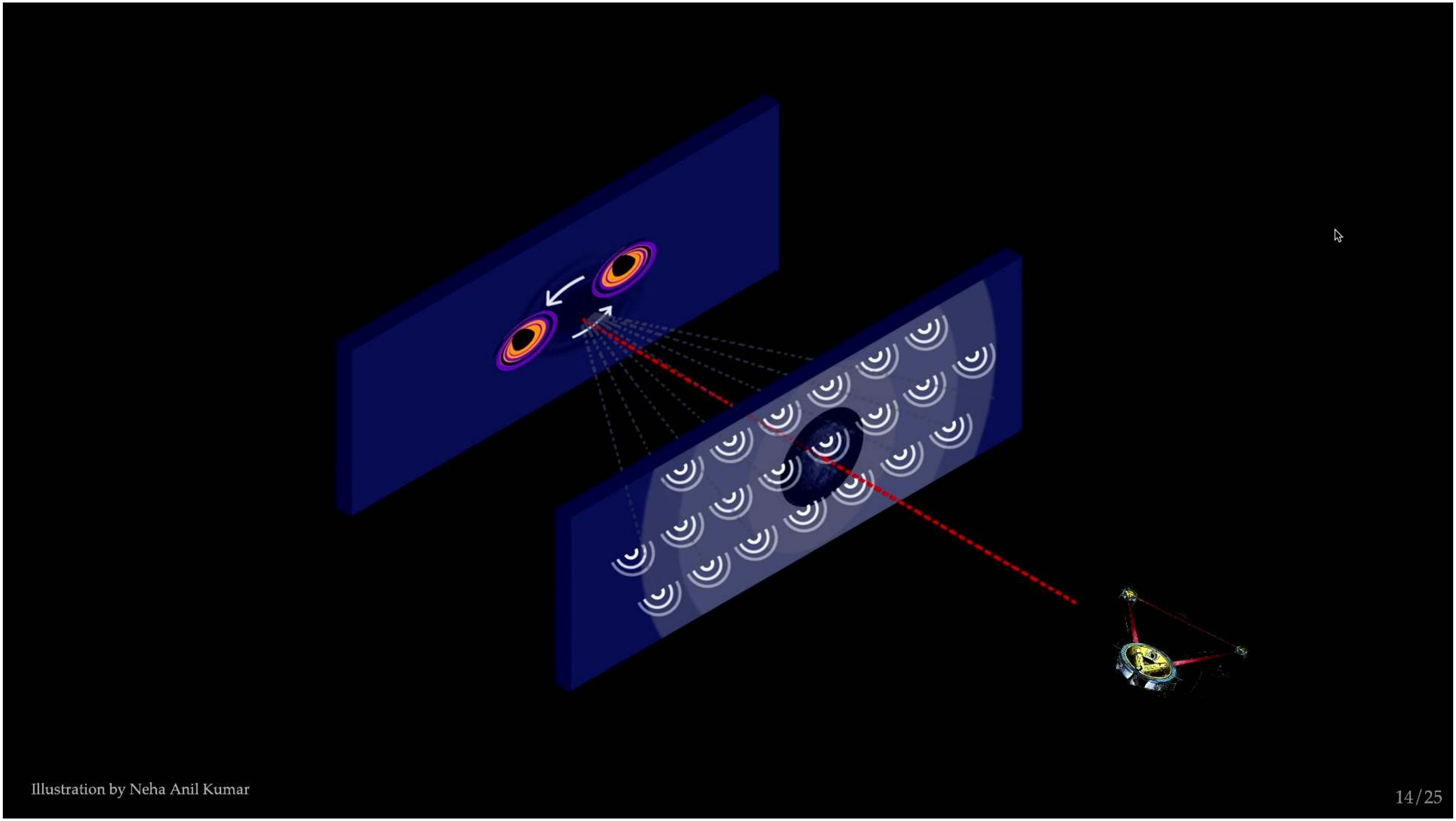
Illustration by Neha Anil Kumar
14/25

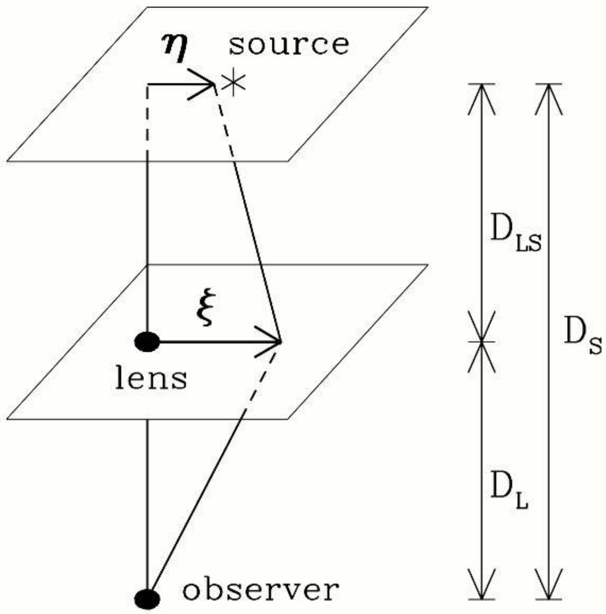

$$\boldsymbol{x} \equiv \frac{\boldsymbol{\xi}}{\xi_0} \qquad \text{and} \qquad \boldsymbol{y} \equiv \boldsymbol{\eta}\frac{D_{\rm L}}{\xi_0 D_{\rm S}}$$

Impact Parameter

Einstein Radius

- $F(f,\boldsymbol{y}) = \dfrac{D_{\rm S}(1+z_{\rm L})\xi_0^2}{D_{\rm L}D_{\rm LS}}\dfrac{f}{i}\displaystyle\int d^2\boldsymbol{x}\,\exp[2\pi i f t_{\rm d}(\boldsymbol{x},\boldsymbol{y})]$
- $t_{\rm d}(\boldsymbol{x},\boldsymbol{y}) = \dfrac{D_{\rm S}\xi_0^2}{D_{\rm L}D_{\rm LS}}(1+z_{\rm L})\left[\dfrac{1}{2}|\boldsymbol{x}-\boldsymbol{y}|^2 - \psi(\boldsymbol{x}) + \phi(\boldsymbol{y})\right]$
- $w = 8\pi M_{\rm Lz} f$

Deflection Potential

(Based on the Matter Distribution of the Lens)

Lensed Waveform in the Frequency Domain: $\tilde{h}^L(f;w,y) = F(w,y)\tilde{h}(f)$

Geometrical optics limit: frequency-independent magnification, time delay, and phase shift

Wave optics effects: frequency-dependent modulations in the amplitude and phase of the waveform (directly dependent on the profile and mass of the lens)

[1] Takahashi and Nakamura (2003)

Lensing of Gravitational Waves

- The wavelength of GWs can be comparable to the size of the lenses, leading to ***frequency-dependent* modulations in the waveform phase and amplitude** due to wave-optics (WO) effects.

- This allows for the possibility of **infer the lens properties** from a single GW observation.

- WO effects can lead to **lensing detectability with cross sections larger than those achievable with the observation of multiple "images."**

[1] Takahashi and Nakamura (2003)
[3] **Çalışkan** et al. (2023a)
[4] **Çalışkan**, et al. (2023b)
[5] Tambalo et al. (2022)
[6] Fairbairn et al. (2022)
[7] Savastano et al. (2023)
[8] Ji and Dai (2024)
[9] Leung et al. (2023)
[10] Dai et al. (2018)
Also:
[11] Feldbrugge, Pen, and Turok (2023)
[12] Feldbrugge and Turok (2020)
[13] Jow and Pen (2022)
[11] Jow and Pen (2024)
[12] Villarrubia-Rojo et al. (2024)

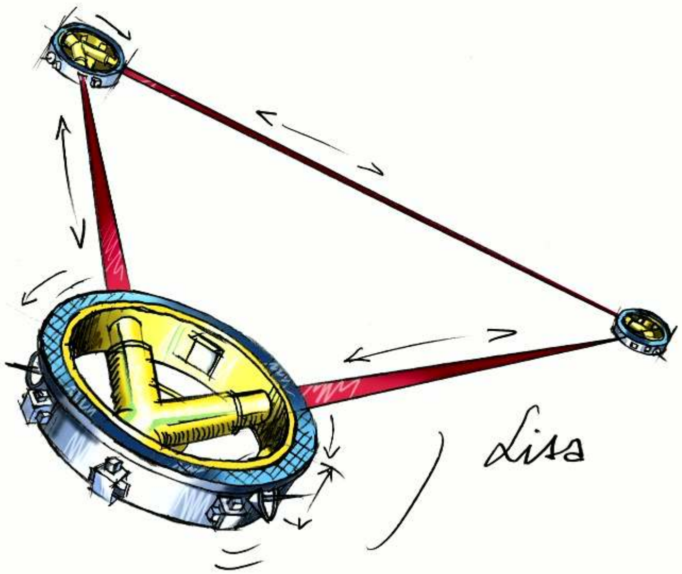

Laser Interferometer Space Antenna (LISA)

- LISA will be the first dedicated space-based gravitational-wave observatory.
- LISA will detect gravitational waves (GWs) emitted by massive black hole binaries (MBHBs) in the low-frequency (~mHz) band.
- These MBHBs ($M_{\mathrm{Total}} \approx 10^4 - 10^8\, M_{\odot}$) will have high SNRs and large redshifts.
- Low-mass lenses, such as dark-matter (DM) subhalos, have sizes comparable to the wavelength of these GWs.

As such, MBHBs are excellent candidates for observing WO effects.

[Credit:] ESA-C. Vijoux

Lensed and Unlensed Waveforms

$$\tilde{h}^L(f; w, y) = F(w, y)\tilde{h}(f)$$

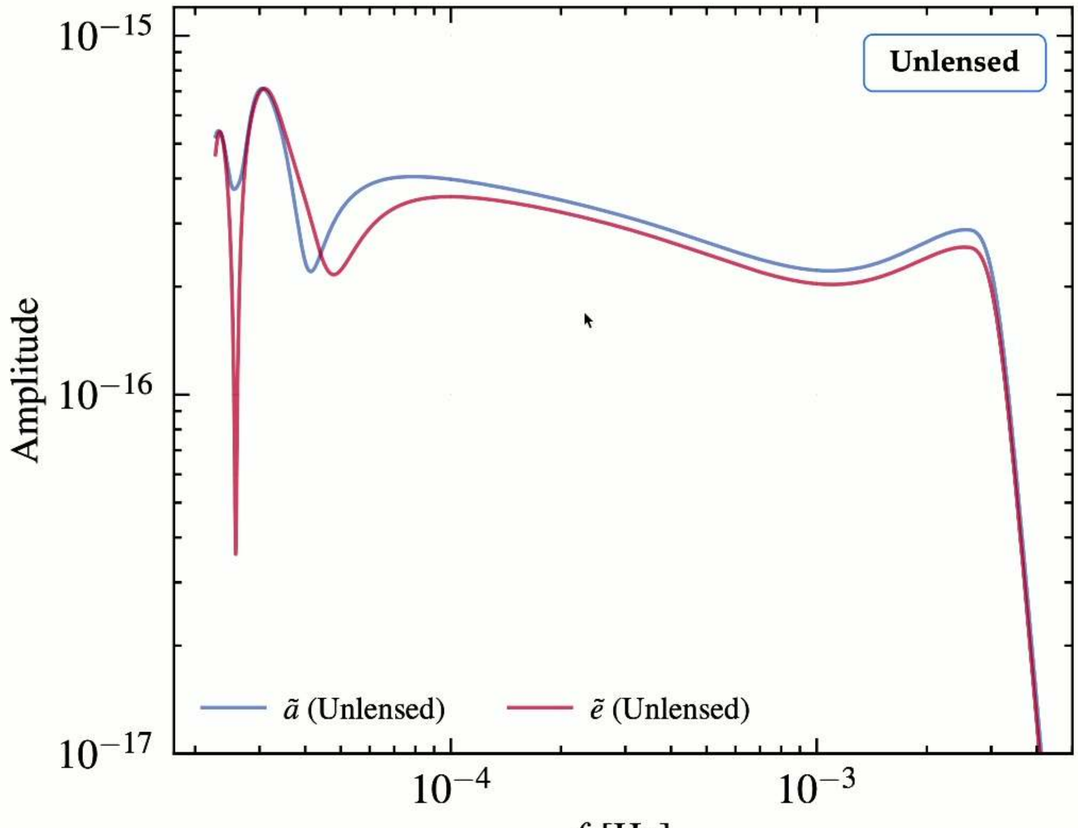

[3] **Çalışkan** et al. (2023a)

Measurability of Lens Mass (M_{Lz})

Measurability of Alignment (y)

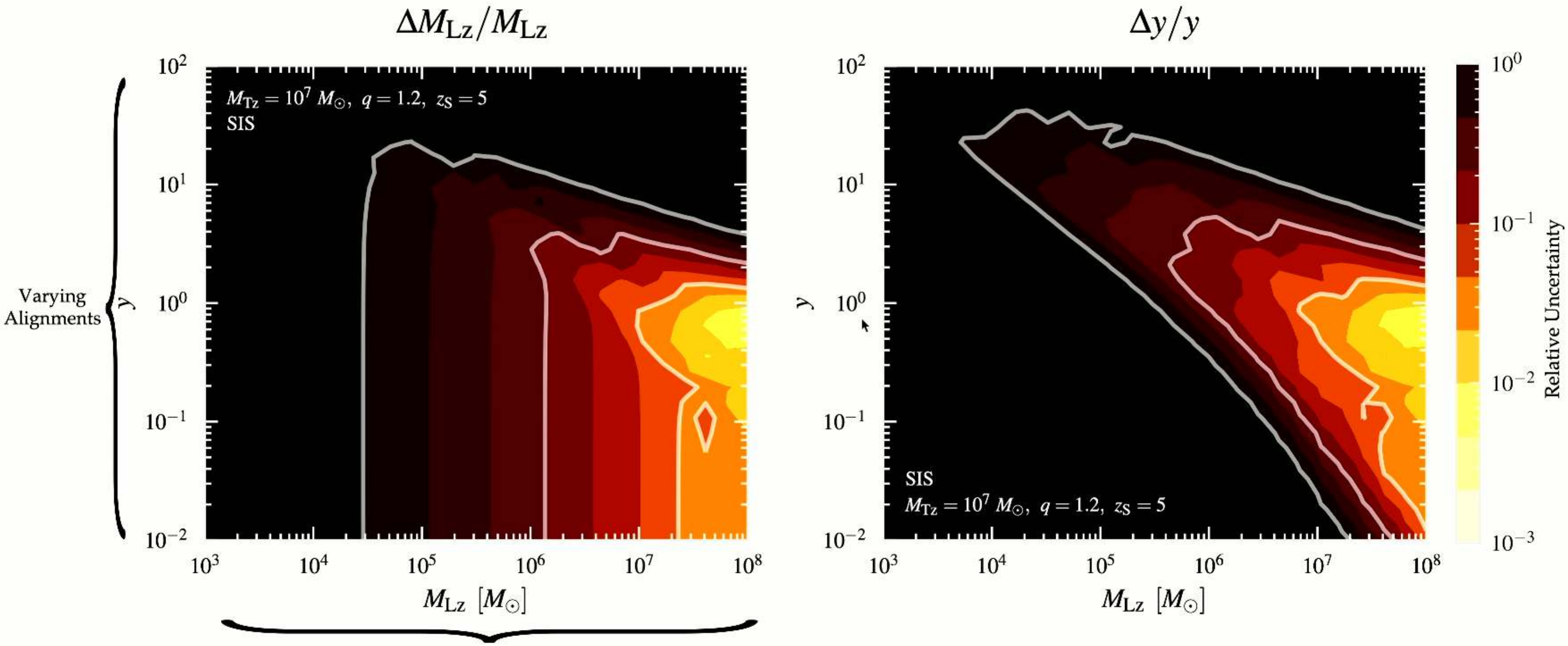

Varying Dark Matter Halo (Lens) Masses

[3] **Çalışkan**, et al. (2023a)
[4] **Çalışkan**, et al. (2023b)

Optical Depth and Probability

Set of Source Parameters **Halo Virial Mass**

$$\tau(\boldsymbol{\theta}^{\mathrm{S}}=\{z_{\mathrm{S}},\dots\}) = \int_0^{z_{\mathrm{S}}} \mathrm{d}z_{\mathrm{L}} \int_{M_{\mathrm{L}}^{\min}}^{M_{\mathrm{L}}^{\max}} \mathrm{d}M_{\mathrm{L}}\, \frac{4\pi M_{\mathrm{L}} D_{\mathrm{LS}}}{D_{\mathrm{L}} D_{\mathrm{S}}}\, y_{\mathrm{cr}}^2(M_{\mathrm{L}}|\boldsymbol{\theta}^{\mathrm{S}})\, n\left[M_{200}, z_{\mathrm{L}}, z_{\mathrm{S}}\right] \chi^2(z_{\mathrm{L}}) \frac{\mathrm{d}\chi(z_{\mathrm{L}})}{\mathrm{d}z_{\mathrm{L}}} \frac{\mathrm{d}M_{200}}{\mathrm{d}M_{\mathrm{L}}}$$

Source Redshift **Lens Redshift** **Lens Mass** **Critical Impact Parameter** **Comoving Number Density of Halos** **Comoving Distance**

$$P = 1 - e^{-\tau(\boldsymbol{\theta}^{\mathrm{S}}=\{z_{\mathrm{S}},\dots\})}$$

[4] **Çalışkan,** et al. (2023b)
[2] Schneider et al. (1992)

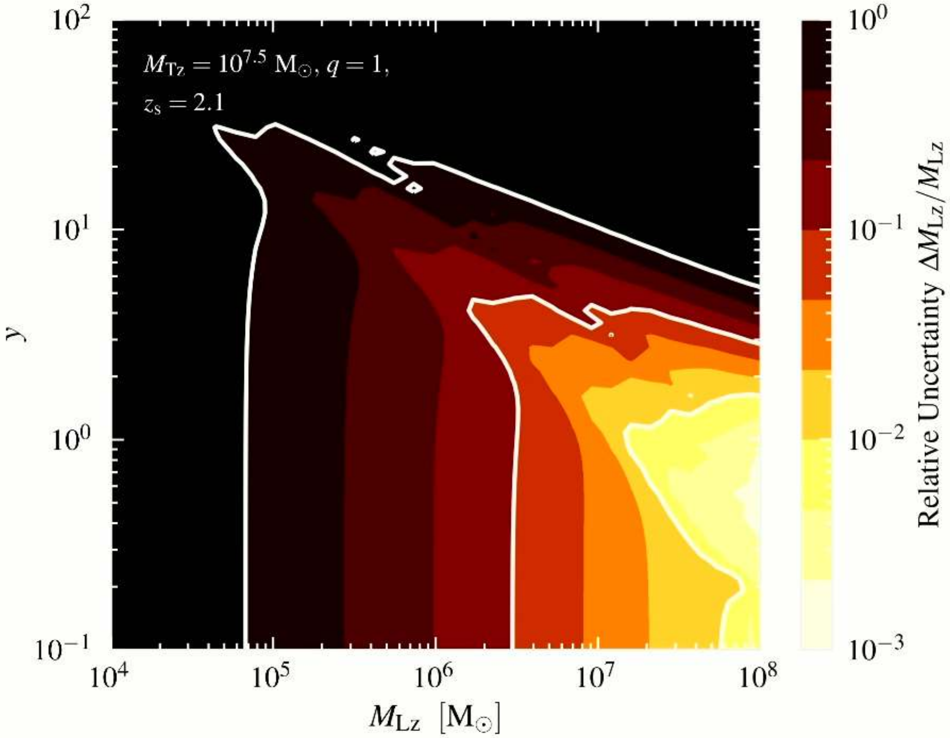

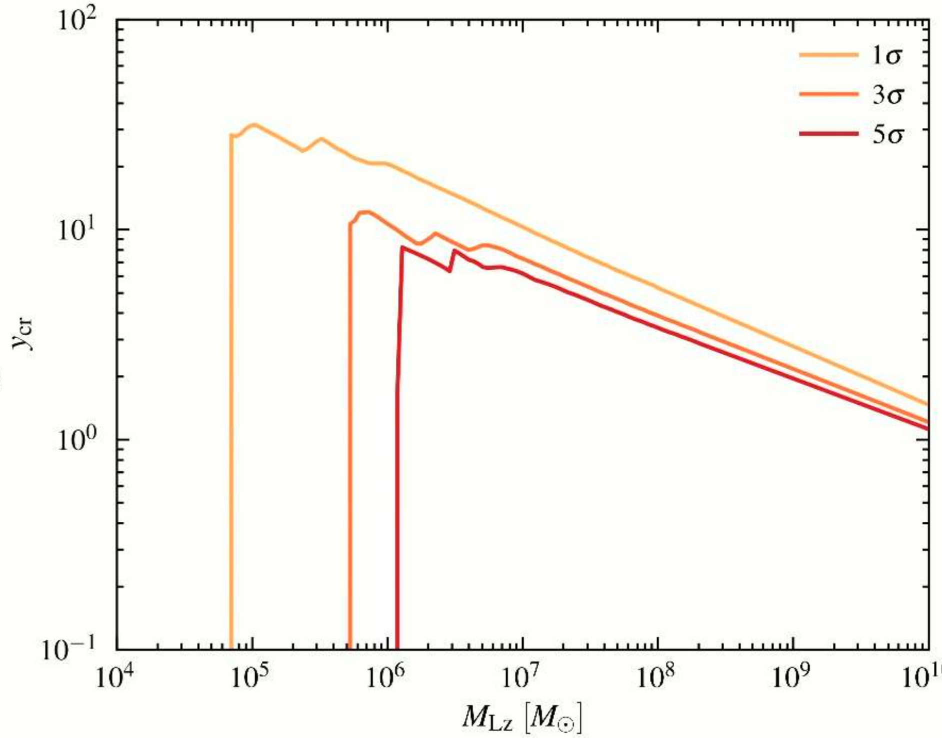

[3] **Çalışkan**, et al. (2023a)
[4] **Çalışkan**, et al. (2023b)

Differential Optical Depth (Probability)

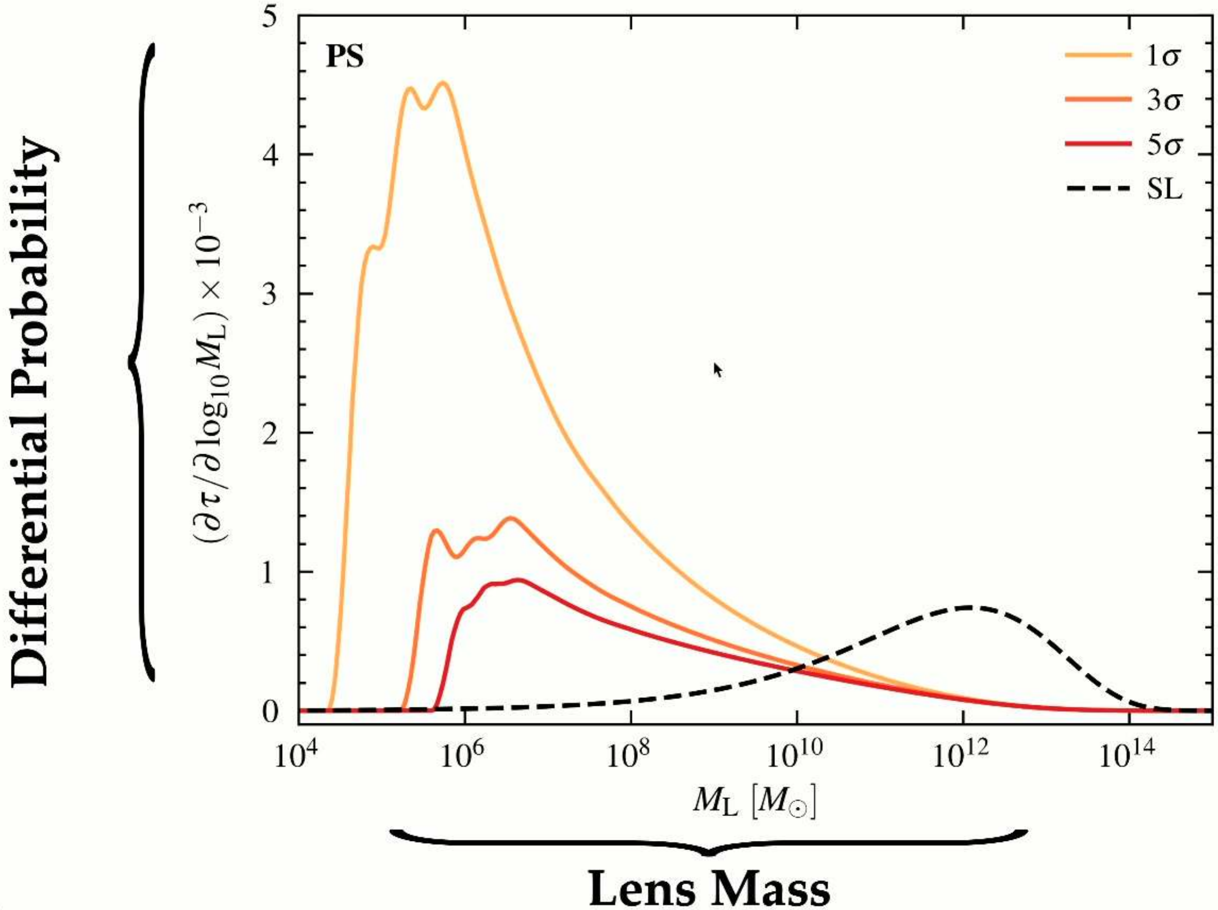

[3] **Çalışkan**, et al. (2023a)
[4] **Çalışkan**, et al. (2023b)

Detection Probability (Source Model Agnostic)

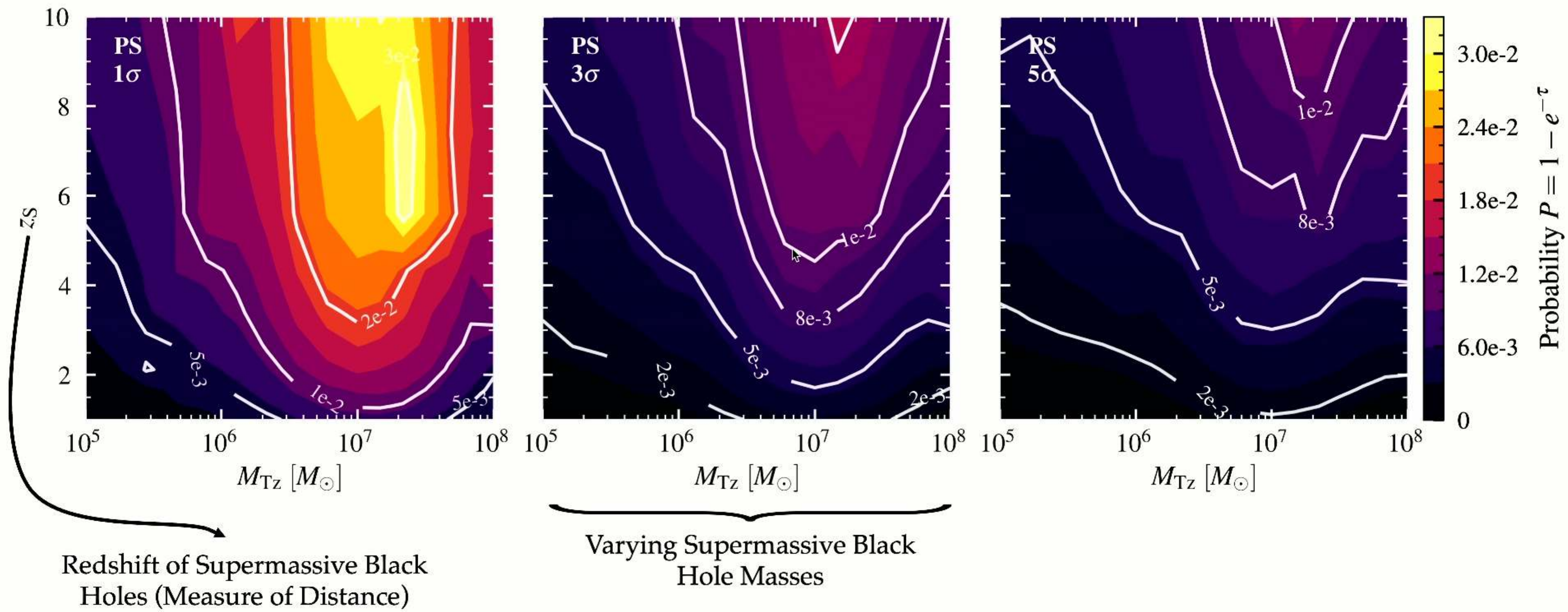

[4] **Çalışkan**, et al. (2023b)

Red MBHBs Are Below Individual Detection Threshold

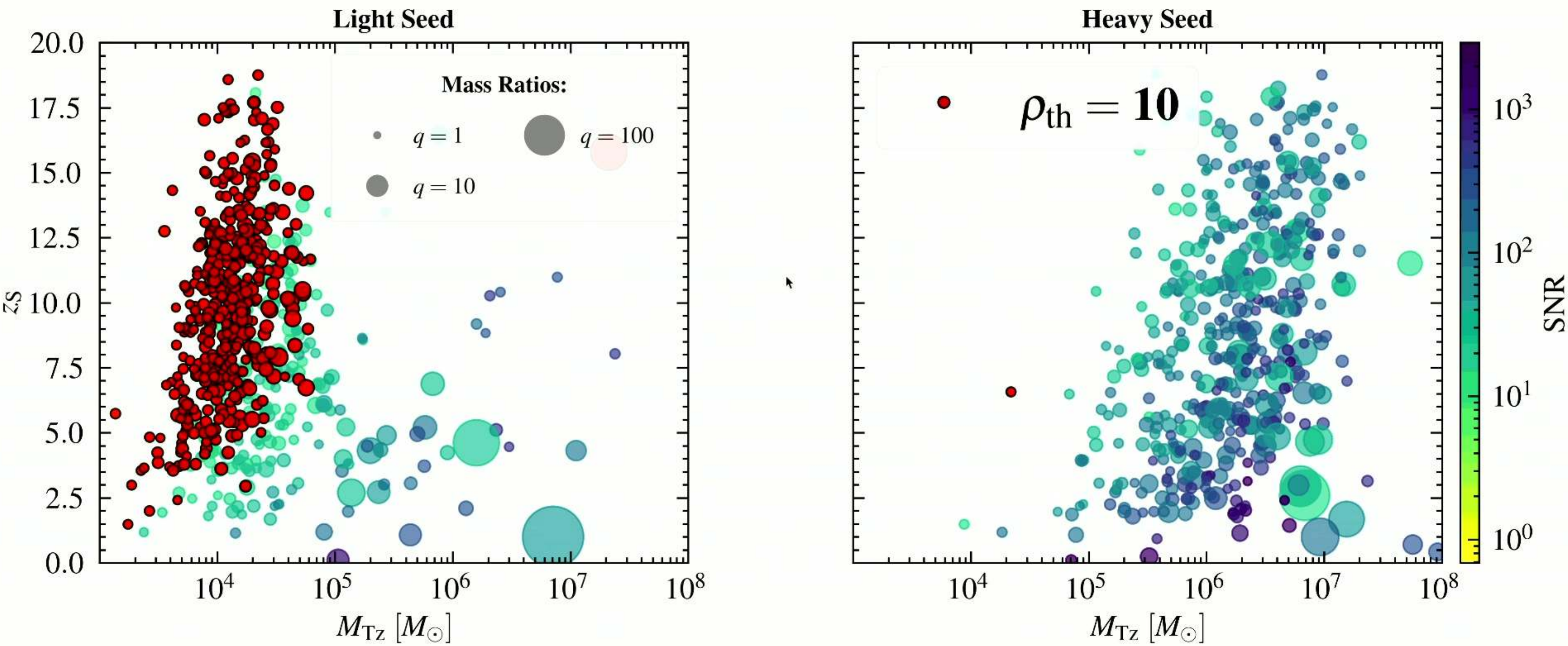

[Adopted from **Çalışkan**, et al. (2023) | Populations Based on Barausse, et al. (2023)]

GW231123

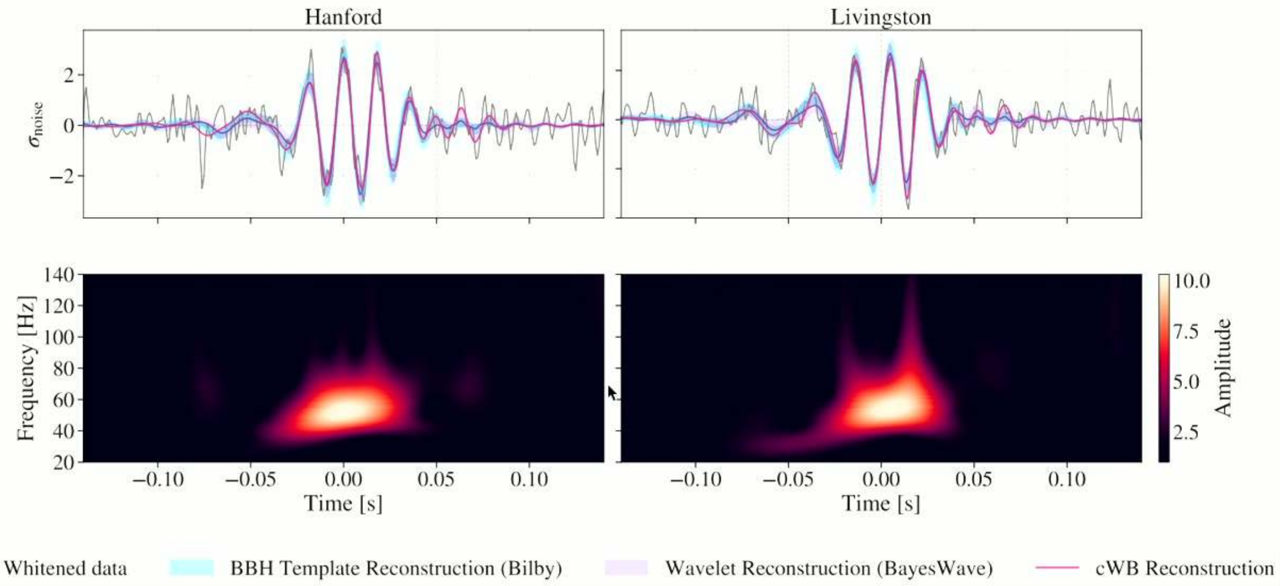

Figure 1. The GW event GW231123 as observed by the LIGO Hanford (left panels) and LIGO Livingston (right panels) detectors. Time is measured relative to 2023 November 23 at 13:54:30.619 UTC. The top panels show the time-domain strain data (black), sampled at 1024 Hz, whitened and then bandpass-filtered with a passband from 20 Hz to 256 Hz (Abbott et al. 2020a). Also shown are the point-estimate whitened waveform from the cWB-BBH search (red), the 90% credible interval of whitened waveforms inferred from a coherent Bayesian analysis using the combined samples from five BBH waveform models (blue bands), and the 90% credible interval inferred from BayesWave using a generic wavelet-based model (shaded purple). The vertical axis is in units of the noise standard deviation, $\sigma_{\rm noise}$. The bottom panels display the corresponding whitened time-frequency representations of the strain data, obtained using a continuous wavelet transform (CWT) with a Morlet–Gabor wavelet. The color scale is in units of the amplitude of the CWT coefficients.

[arXiv: 2507.08219, LVK]

GW231123

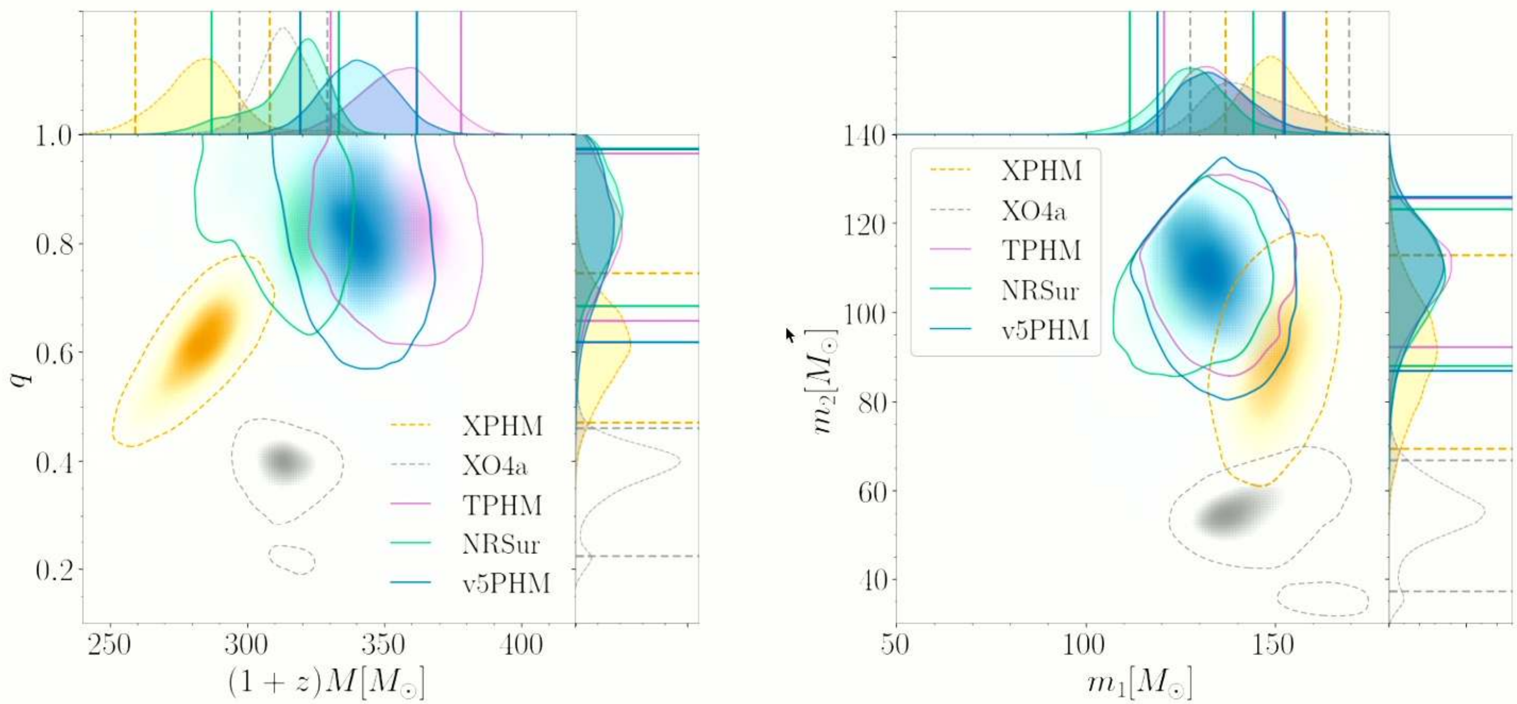

Figure 7. Marginalized posterior probability for the *Left*: redshifted (detector-frame) total binary mass and the mass ratio, and *Right*: primary and secondary source-frame masses inferred from GW231123 for each of the five models considered. Each contour, as well as the colored horizontal and vertical lines, shows the 90% credible intervals.

[arXiv: 2507.08219, LVK]

5 Cycles

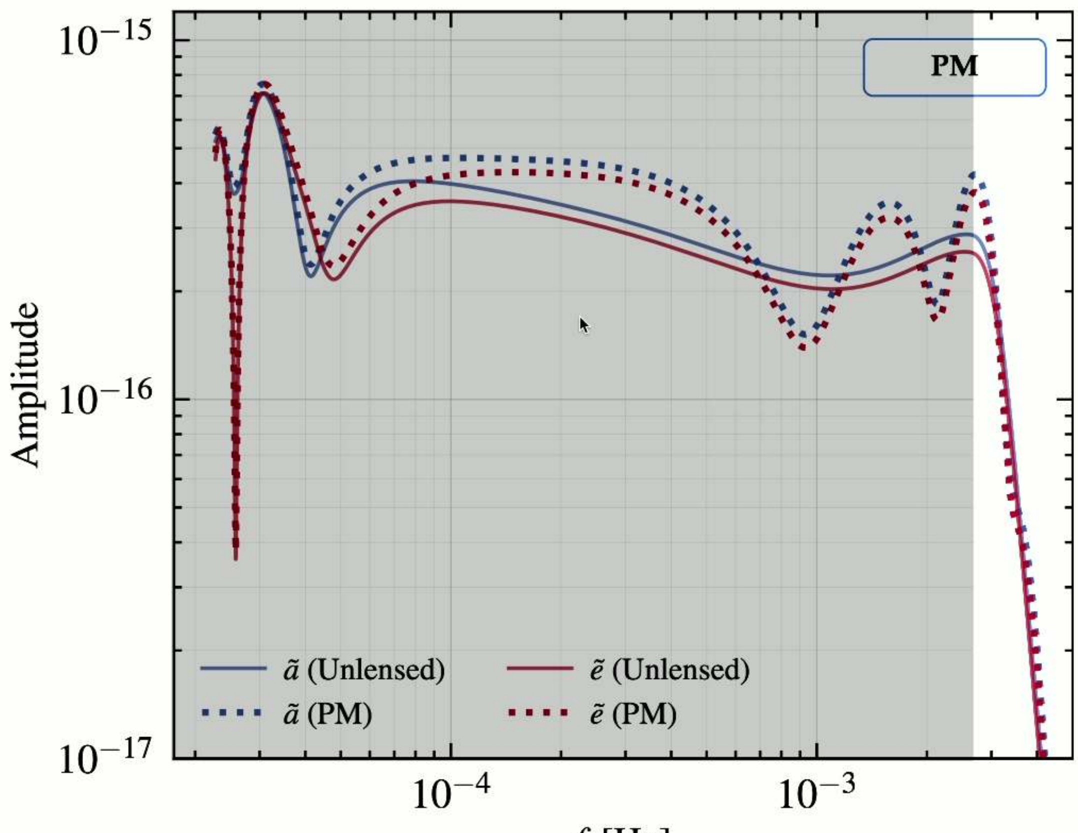

[3] **Çalışkan** et al. (2023a)

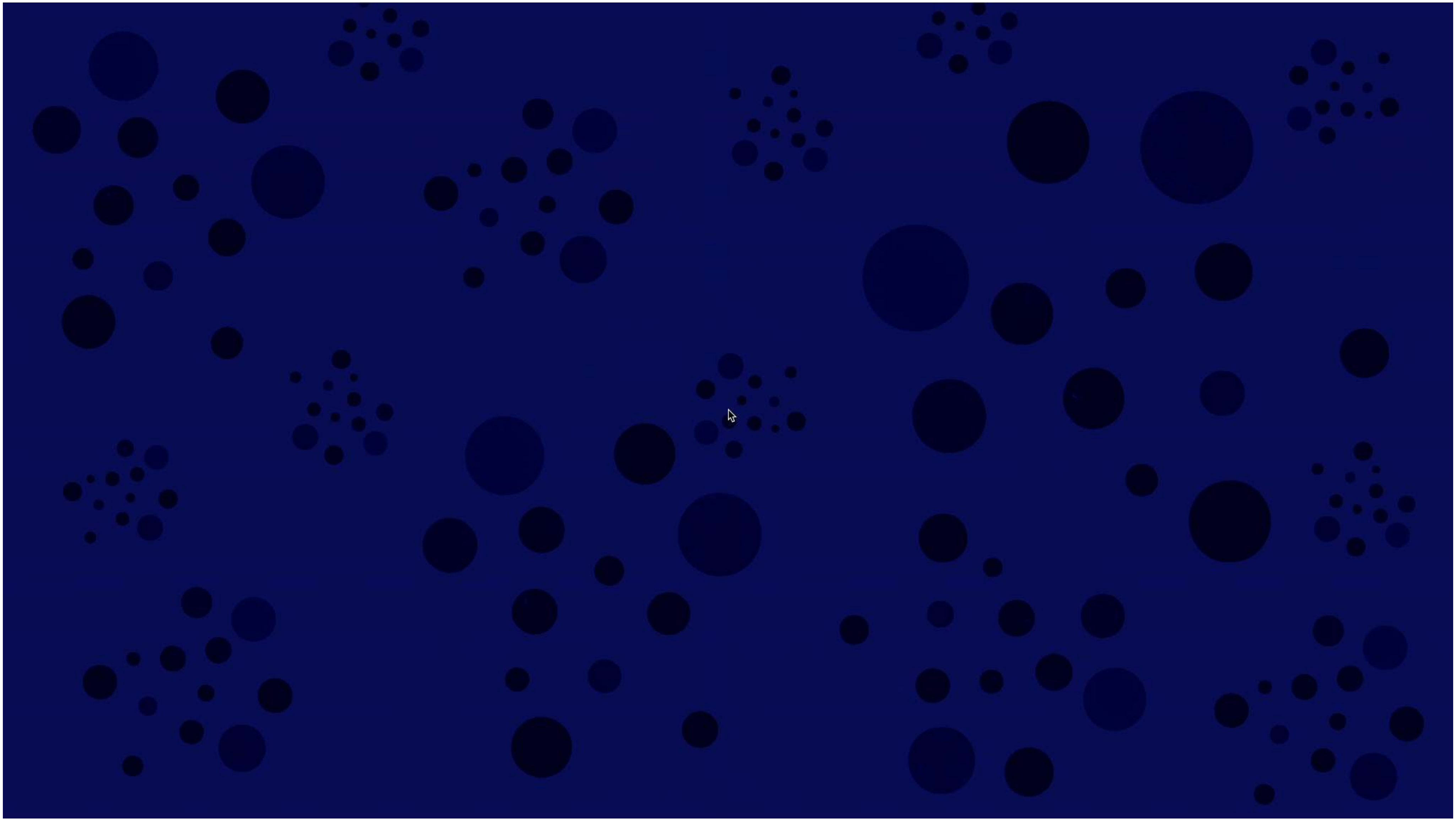

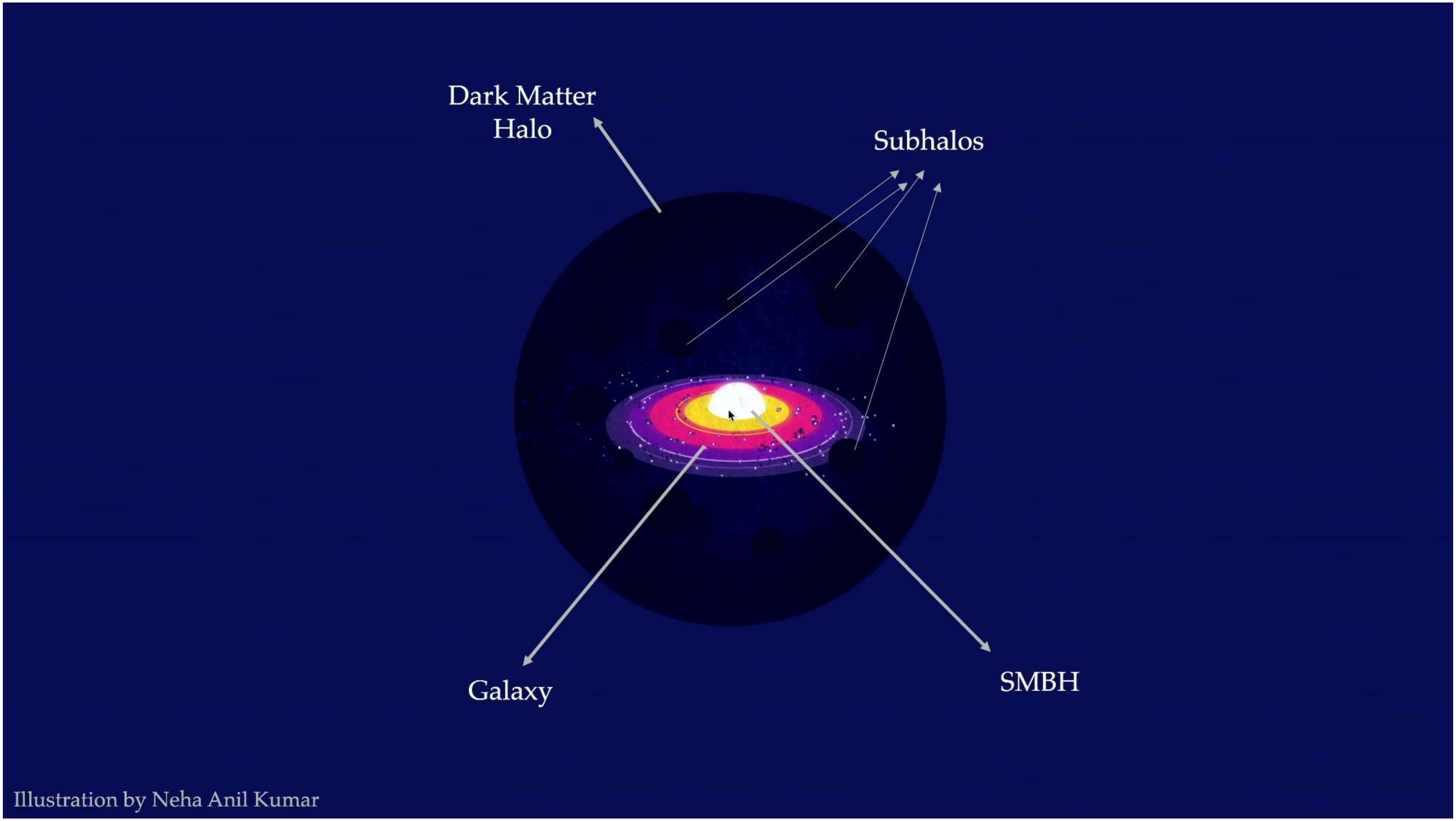
Dark Matter
Halo
Subhalos
Galaxy
SMBH
Illustration by Neha Anil Kumar